Theoretical Survey of the Potential Energy Surface of Ti^+ + Methanol Reaction

Fengyun Zhang,[†] Wenyue Guo,*[,†] Lianming Zhao,[†] Xianqing Lin,[†] Lizhen Zhang,[†] Houyu Zhu,[†] and Honghong Shan*[,‡]

College of Physics Science and Technology and State Key Laboratory for Heavy Oil Processing, China University of Petroleum, Dongying, Shandong 257061, PR China

Received: February 12, 2009; Revised Manuscript Received: May 7, 2009

The gas-phase reaction of Ti^+ (^4F and ^2F) with methanol is investigated using density functional theory. Geometries and energies of the reactants, intermediates, and products involved are calculated. The approach of Ti^+ toward methanol could form either a "classical" O- or a "nonclassical" η^3-methyl H-attached complex. The reaction products observed in the experiment (Guo, Kerns, Castleman *J. Phys. Chem.* **1992**, *96*, 4879) are produced via the classical association rather than the nonclassical complex. All possible pathways starting with C−O, C−H, and O−H activation are searched. Methane and methyl loss products (TiO^+ and $TiOH^+$) are produced via the C−O activation; the O−H activation accounts for the H_2 and H elimination (producing $TiOCH_2^+$ and $TiOCH_3^+$); and the C−H activation is unlikely to be important. Through the bond insertion (H shift) reductive elimination mechanism, the products of a closed-shell molecule (H_2 or methane) elimination could take place on both the quartet and doublet PESs owing to a spin inversion occurring in the course of initial bond insertion, whereas only the quartet products are produced adiabatically via the simple bond insertion−reductive elimination mechanism for the loss of a radical-type species (H or CH_3). The computational results are in concert with the available experimental information and add new insight into the details of the individual elementary steps.

1. Introduction

The reaction of "naked" transition-metal cations with alcohols in the gas phase has been extensively investigated over the past three decades owing to its fundamental importance in catalysis, oxidation, and material synthesis.[1−12] Because it is the simplest aliphatic alcohol as well as one of the most important industrial synthetic raw materials, much attention has especially been paid to the chemistry of methanol.[3−5,7−11] By using ion cyclotron resonance (ICR) spectrometry, Allison and Ridge reported that Fe^+ reaction with methanol gives $FeOH^+ + CH_3$, whereas neither Co^+ nor Ni^+ reacts with methanol.[3] However, results of Fourier transform mass spectroscopy (FTMS) suggested that both Fe^+ and Cr^+ are unreactive to methanol, whereas Mo^+ affords $Mo(CH_2O)^+ + H_2$.[4] By using FTMS, Weil and Wilkins demonstrated that Au^+ predominantly affords $AuH + CH_2OH^+$ via reaction with methanol, whereas Cu^+ exclusively gives the $Cu(CH_3OH)^+$ addition.[5] The Fourier transform ICR (FT-ICR) study showed that reaction of M^+ (M = V, Nb, and Ta) with CH_3OH accounts for the dominant products of MO^+ and MOH^+, accompanied by fewer $NbOCH_2^+$ and $VOCH_3^+$.[9]

Although experimental works are very extensive, it still remains open to address the mechanistic details of the reaction of transition-metal ions with primary alcohols. A complete characterization of the actual reaction mechanism as well as the relevant intermediates needs a close collaboration between experiment and theory. Surprisingly, theoretical works dedicated to this respect are still relatively scarce. Cao et al.[9] have reported the potential energy surfaces (PESs) of the oxidation of M^+ (M = V, Nb, and Ta) by CH_3OH using the B3LYP/LANL2DZ+6-31G* protocol, in which the oxidation to MO^+ was found to occur through M^+ insertion into the C−O bond, followed by a hydroxyl H shift and then an elimination dissociation and a spin inversion occurring after the C−O activation transition state was suggested to play an important role in decreasing barrier heights for the following steps. Theoretical study employing density functional theory (DFT), Hartree−Forck, Møller−Plesset perturbation, and Guassian methods confirmed that $Al^+(^1S)$ reaction with ethanol yields $Al(H_2O)^+$ and ethylene as the dominant products at thermal energies.[12] Three distinct reaction pathways were taken into account, that is, oxidative-addition and reductive-elimination, oxidative addition followed by 1,4-H shift, and electrophile-inducted one-step syn-elimination, and the last one of them was found to be energetically the most favorable.[12] Methane-to-methanol conversion by various first-row transition-metal oxide ions including TiO^+ was reported to proceed through direct H abstraction to form intermediate $(CH_3)Ti^+(OH)$ followed by methyl migration, with a spin inversion occurring before the transition state of the latter step at the B3LYP/6-311G** level.[13]

In this article, we report a comprehensive theoretical study of the Ti^+ + methanol reaction using DFT. This reaction has been investigated using the selected ion drift tube technique coupled to a laser vaporization source (SIDT-LV), and multiple products of $TiOH^+$, TiO^+, $TiOCH_2^+$, and $TiOCH_3^+$ were observed.[10] The products associated with the H, CH_3, and CH_4 elimination were also found for the reaction of Ti^+−methanol heteroclusters using the laser ablation−molecular beam (LA−MB) method, and the H-elimination was suggested to involve O−H bond activation by isotope-labeling experiments.[11] These results suggest that Ti^+ is very active toward breaking C−H, O−H, and C−O bonds in methanol. The objective of this article is to determine the useful mechanistic details and activation barriers to give insight into the kinetic aspects for the title reaction. This includes a detailed illustration of all possible competing

* To whom correspondence should be addressed. E-mail: wyguo@hdpu.edu.cn (W.G.); shanhh@hdpu.edu.cn (H.S.).
† College of Physics Science and Technology.
‡ State Key Laboratory for Heavy Oil Processing.

10.1021/jp901326r CCC: $40.75
Published on Web 05/29/2009

pathways on both quartet and doublet PESs as well as an estimation of the crossing possibility between the high- and low-spin surfaces where it is needed. Indeed, spin inversion has been suggested to play an important role in the reaction of small organic molecules with early transition-metal ions, such as Sc^+, Ti^+, V^+, and so on.[9,13−19]

2. Computational Methods

Geometries of all of the involved species on both the quartet and doublet PESs were fully optimized using the hybrid B3LYP[20,21] functional in conjunction with the DZVP basis set[22] for Ti and the 6-311++G(2df,2p) basis for the remaining atoms. This selected method has been proven to combine reasonable computational cost with accuracy sufficient for describing open-shell metal systems.[23] Frequency calculations were performed at the same level to evaluate zero-point energies (ZPEs) and to determine whether the optimized species is a minimum or a saddle point. Scaling factor for the ZPEs was selected to be 0.961. The optimized transition states were also confirmed by intrinsic reaction coordinate (IRC) calculations. With the optimized structures, single-point energies were calculated using the B3LYP method with the DZVP basis set, supplemented with a set of [1s1p1d] diffuse components[24,25] and three sets of uncontracted pure angular momentum f functions, for Ti and the 6-311++G(2df,2p) basis set for C, H, and O (noted as BSI for the basis sets).[26] In a recent work,[18] we have shown the performance of this computational strategy for describing the features of the PESs of Ti^+/oxo-organic molecules.

To locate the minimum energy crossing point (MECP) between the quartet and doublet surfaces for a step considered, single-point energies of both the states were calculated at the B3LYP/BSI level for the relevant IRC points along the quartet pathway until they have an equal energy. All of these calculations were performed using the Gaussian 03 package.[27]

Spin−orbit coupling (SOC) at the MECP was calculated with the GAMESS package.[28] CASSCF calculations with the DZVP basis set[22] for Ti and the 6-311G basis for the remaining atoms were first performed to get the converged CASSCF wave functions for both states at the MECP. The SOC matrix elements were then computed using the SOC−CI method.[29] Because the orbital sets of both states must share a common set of frozen core orbitals in the SOC matrix elements calculations, the converged CASSCF wave functions of the doublet state were employed as a reference state for both the quartet and doublet CI wave functions. The one-electron effective spin−orbit operator was used as eq 1[29]

$$\mathbf{H}_{SO} = \frac{\alpha^2}{2}\sum_i \sum_k \left(\frac{Z_k^*}{r_{ik}^3}\right)\mathbf{S}_i\cdot\mathbf{L}_{ik}, \quad \frac{\alpha^2}{2} = \frac{e^2h}{4\pi m_e^2 c^2} \tag{1}$$

where $\mathbf{L}_{ik}$ amd $\mathbf{S}_i$ are the orbital and spin angular momentum operators, respectively, for electron i in the framework of nuclei indexed by k. The effective nuclear charge, Z_k^*, is an empirical parameter in the one-electron spin−orbit Hamiltonian. Z* is 3.9, 5.6, and 9.6 for carbon, oxygen, and titanium, respectively.[30]

The SOC value is the matrix element that expresses the coupling of the quartet and doublet states by the operator of eq 2

$$\langle \mathbf{H}_{SO}\rangle_{S,S'} = \langle {}^4\Psi_1(\mathbf{M}_S)|\mathbf{H}_{SO}|{}^2\Psi_2(\mathbf{M}_{S'})\rangle \tag{2}$$

Here ${}^4\Psi_1$ (${}^2\Psi_2$) is the $\mathbf{M}_S$ ($\mathbf{M}_{S'}$) component of the many-body quartet-state (doublet state) wave function. Considering the generated spin sublevels $\mathbf{M}_S$, a reasonable measure of the SOC-induced quartet-doublet interaction is the root-mean-square coupling constant (SOCC) of eq 3

$$\mathrm{SOCC} = \left[\sum_{S,S'} \langle \mathbf{H}_{SO}\rangle_{S,S'}^2\right]^{1/2} \tag{3}$$

A crude estimation of the crossing probability at the MECP can be done using the Landau−Zener formula[31]

$$P = 1 - e^{-2\delta}, \quad \delta = \frac{\pi|V_{ij}|^2}{\hbar v|\Delta g_{ij}|} = \frac{\pi|\mathrm{SOCC}|^2}{(2\min(S_i, S_j) + 1)\hbar v|\Delta g_{ij}|} \tag{4}$$

where V_{ij} is a matrix element of a diabatic operator (SOC in this case) coupling two adiabatic states i and j, Δg_{ij} is the difference in the gradients of the two adiabatic states i and j, and v is the effective velocity with which the system is passing through the crossing point that can be calculated from the kinetic theory of gases at 298 K.

We also made use of the natural bond orbital (NBO) theory to characterize the bonding characters between different groups for some important species involved. These calculations were performed using the NBO5.0 program package.[32]

3. Results and Discussion

Considering the effects of high- and low-spin electronic states of the metal ion on the reactivity and reaction pathways,[9,13−19] we present here a study of both the quartet and doublet PESs of $[Ti, C, O, H_4]^+$. In the following sections, we first give the structures and energies of the reactants, encounter complexes, and product species involved in the $Ti^+ + CH_3OH$ reaction. Then, we report the theoretical results of the reaction channels starting with C−O, O−H, and C−H activation in turn, including geometries for all relevant species, PES profiles for all possible product channels, and crossing possibility between different spin PESs for some important steps. Lastly, we give the reaction mechanisms by comparing our theoretical results with the experimental findings.[10,11] For simplicity, calculated energies and zero point energies for all relevant species are given as Supporting Information. (See Table S1.)

3.1. Reactants, Encounter Complexes, and Product Species. In this section, we discuss calculated structures and energies for the reactants, encounter complexes, and product species relevant to the Ti^+ + methanol reaction. The resulting structures are given in Figure 1. Table 1 tabulates calculated bond dissociation energies (BDEs) and excitation energies (EEs) for these species.

The structure of methanol has been widely investigated both experimentally[33] and theoretically.[34] In the present study, methanol is also optimized, and the resulting structure is shown in Figure 1 together with the experimental structural parameters.[33] Good agreement between calculation and experiment can be found. It is known that DFT calculations can properly describe ground states, even for transition-metal systems, and also that this method gives good results for some excited-state calculations.[15] For the Ti^+ system, the doublet state is a three-electron doublet state, which can be formed through various orbital occupations. Therefore, it is difficult to describe properly with single-determinant methods. However, the results from the

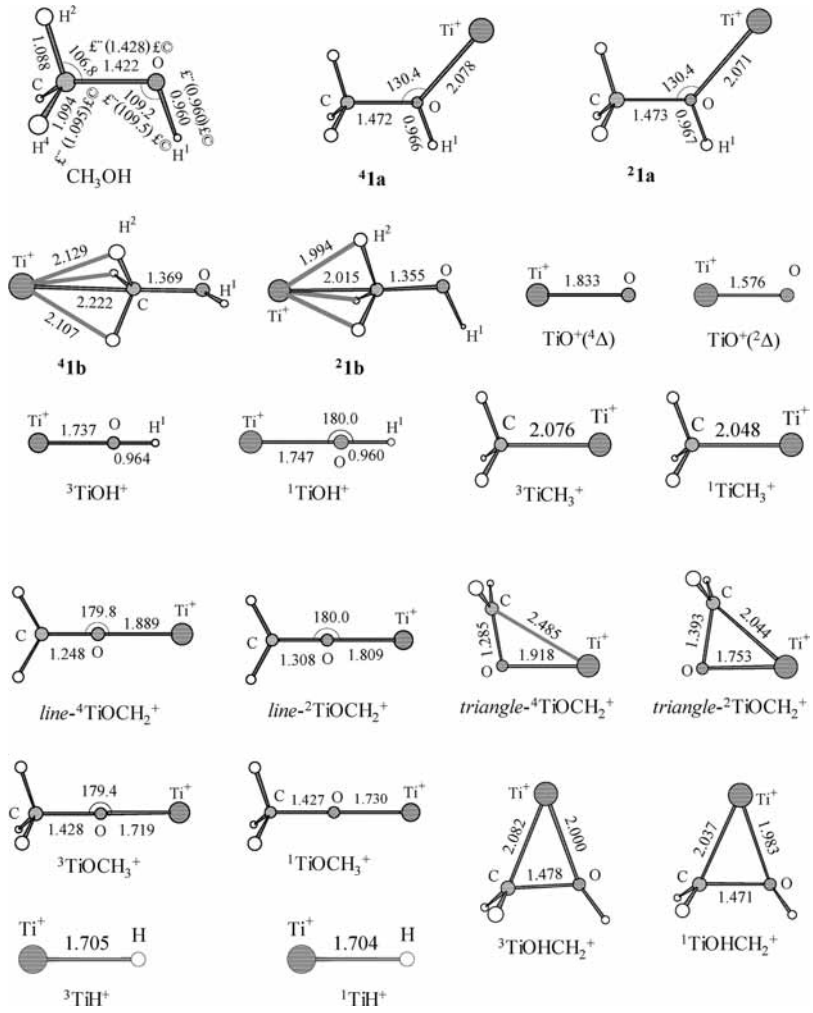

Figure 1. Geometries and selected structural parameters optimized at the B3LYP/DZVP+6-311++G(2df,2p) level for reactant, encounter complexes, and product species involved in the Ti^+ + methanol reaction. Parameters in parentheses are experimental values taken from ref 33. Bond lengths are in angstroms, and bond angles are in degrees.

TABLE 1: Calculated Bond Dissociation Energies (BDEs) and Excitation Energies (EEs) (in kilocalories per mole) for Ti^+ and Ti^+ Complexes with Methanol and Other Relevant Species at the B3LYP/BSI//DZVP+6-311+G(2df,2p) Level

	BDEs[b]		
species[a]	high-spin state	low-spin state	EEs
Ti^+			13.0 (13.03[c])
classical-Ti−$OHCH_3^+$	48.4 (51.0[d])	27.7 (40.9[d])	20.7 (10.1[d])
nonclassical-Ti−$OHCH_3^+$	10.2	3.9	6.3
Ti^+−O	82.6	155.5 (155.1,[d] 159.7,[e])	72.9 (80.7,[f] 71.7[g])
Ti^+−OH[h]	115.3 (111.2,[i] 116.3[j])	68.9	46.4
Ti^+−CH_3[h]	60.7 (57.5[k])	32.3	28.4
line-Ti^+−OCH_2	51.2	33.9	17.3
triangle-Ti^+−OCH_2	42.0	55.1	13.1
Ti^+−OCH_3[h]	109.4	82.2	27.2
Ti^+−$OHCH_2$[h]	71.9	46.6	25.3
Ti^+−H[h]	60.2 (54.2[k])	28.6	31.6

[a] High- and low-spin states of the species are quartet and doublet states, respectively, unless otherwise indicated. [b] Values are relative to the total energy of $Ti^+(^4F)$ and the relevant species. [c] Ref 35. [d] Values calculated at the B3LYP/6-311G** level; ref 13. [e] Experimental value; ref 36. [f] Experimental value; ref 37. [g] Values calculated at the B3LYP/TZVP+G(3df,2p) level; ref 15. [h] High- and low-spin states for these species are triplet and singlet states, respectively. [i] Experimental value; ref 38. [j] B3LYP value; ref 39. [k] Experimental value; ref 40.

present B3LYP calculations are reasonably close to experimental observations as mirrored by the fact that the theory can reproduce the Ti^+ $^2F \leftarrow {}^4F$ energy gap well (13.0 vs 13.03 kcal/mol).[35]

All possible complexes of Ti^+ with CH_3OH are considered, and two types of encounter isomers, that is, "classical" O attached complex (**1a**) and "nonclassical" methyl-H attached complex (**1b**), are found. (See Figure 1.) In complex **1a** (C_s), Ti^+ is attached at the O atom of CH_3OH with the Ti^+−O distance being 2.078 (quartet) and 2.071 (doublet) Å and the Ti^+−O−C angle being 130.4°. Owing to electron donation from the O lone pair orbitals to the metal center, the association stretches the O-containing bonds (O−C bond: by ∼3.5%; O−H bond: by ∼0.7%) and thus weakens the bonds. The weakened

bonds are expected to be easily activated by the metal ion giving different products, as discussed below. This type of association accounts for relatively large binding energies (48.4 and 27.7 kcal/mol for the quartet and doublet states, respectively, compared with 51.0 and 40.9 kcal/mol in the previous calculations[13]). Alternatively, the approach of Ti^+ to the methyl end of methanol yields the "nonclassical" η^3-complex **1b**. A striking feature of complex **1b** is the shortening of the C−O bond (by 3.7 (quartet) and 5.4% (doublet)) as well as the stretching of the C−H bonds (by ∼2.8 and ∼5.7%). NBO analysis shows that complex **1b** is stabilized to some extent by electron donations from the σ(CH) bonding orbitals to the metal 4s and 3d orbitals as well as back-donations from the metal to the σ^*(CH) and σ^*(CO) orbitals. This type of association is relatively weak with the BDEs being 10.2 (quartet) and 3.9 (doublet) kcal/mol. Direct conversion between **1a** and **1b** has been carefully searched, but no transition states can be found.

TiO^+ is the methane-elimination product in the reaction of Ti^+ with methanol.[10] As shown in Figure 1, free $TiO^+(^2\Delta)$ has an obviously shorter bond length (1.576 Å) than its quartet analogue (1.833 Å). NBO analysis detects that one σ and two π doubly occupied orbitals are formed in $TiO^+(^2\Delta)$, whereas, in the high-spin state, Ti^+ forms only one doubly occupied σ bonding orbital with the O atom. These facts suggest the Ti^+O bond in the doublet is obviously stronger than that in the quartet (BDEs: 155.5 vs 82.6 kcal/mol). Note that the calculated BDE of $TiO^+(^2\Delta)$ agrees well with those determined both experimentally (159.7 kcal/mol[36]) and theoretically (155.1 kcal/mol).[13] Furthermore, the calculated doublet → quartet excitation energy (72.9 kcal/mol) is a little lower than that estimated by Armentrout and coworkers (80.7 kcal/mol)[37] but agrees well with that calculated at the B3LYP/TZVP+G(3df,2p) level by Ugalde and coworkers (71.7 kcal/mol).[15]

$TiOH^+$ is the major product via methyl elimination in the title reaction.[10] In both high- and low-spin states, the species is featured by a linear structure with the rather large BDE of 115.3 (triplet) and 68.9 (singlet) kcal/mol; the calculated BDE for $^3TiOH^+$ accords well with both the theoretical (111.2 kcal/mol)[38] and experimental (116.3 kcal/mol[39]) values. However, somewhat weaker binding is found for Ti^+CH_3 (BDEs: 60.7 (triplet) and 32.3 (singlet) kcal/mol); note that the calculated value for $^3TiCH_3^+$ agrees well with the experimental finding (57.5 kcal/mol).[40] The weaker Ti^+-CH_3 bond is in keeping with the preferred rupture of the Ti^+−C bond in the C−O insertion species $(CH_3)Ti^+(OH)$, which gives Ti^+OH as the final product, as mentioned below.

The H_2-elimination product is the $TiOCH_2^+$ complex.[10] The attachment of Ti^+ to CH_2O could form either line- or triangle-type association. (See Figure 1.) In the line complex, Ti^+ is located at the C_2 axis of formaldehyde, whereas the metal ion simultaneously binds to both the C and O atoms in triangle-$TiOCH_2^+$. The BDEs of the quartet and doublet line-$TiOCH_2^+$ are 51.2 and 33.9 kcal/mol, whereas they are 42.0 and 55.1 kcal/mol for triangle-$TiOCH_2^+$. Correspondingly, similar to its direct precursor Ti^+, line-$TiOCH_2^+$ has a quartet ground state, whereas for the triangle-complex, the reverse order is correct. NBO analysis suggests that only one singly occupied $\sigma(Ti^+C)$ bonding orbital is formed in the line-type species (α for quartet and β for doublet) as well as for the quartet triangle-$TiOCH_2^+$ complex (α-spin), whereas in the doublet triangle-$TiOCH_2^+$ species formed are the doubly occupied $\sigma(Ti^+C)$, $\sigma(Ti^+O)$, and $\pi(Ti^+O)$ bonding orbitals, explaining the relatively strong bond.

For the H elimination product,[10] two candidates can be envisaged: $TiOCH_3^+$ via initial O−H activation and $TiOHCH_2^+$ via C−H activation. Coordination of Ti^+ to the O atom of CH_3O accounts for the linear-type $TiOCH_3^+$ complex, and a triangle-type $TiOHCH_2^+$ complex is formed because Ti^+ simultaneously attacks both O and C atoms of CH_2OH. (See Figure 1.) In the triplet and singlet states, the BDEs are calculated to be 109.4 and 82.2 kcal/mol for $TiOCH_3^+$ and 71.9 and 46.6 kcal/mol for $TiOHCH_2^+$. The relatively strong Ti^+-OCH_3 bond indicates that products via initial O−H activation are more stable and thus more possible to be produced. For TiH^+, although it has almost equal bond length in both states (1.704 to 1.705 Å), the Ti^+−H bond is much stronger in the triplet state than in the singlet state (BDEs: 60.2 vs 28.6 kcal/mol). The former value is compared with the experimental value of 54.2 kcal/mol.[40]

TABLE 2: Summary of All of the Possible Products and the Relative Energies (E) (in kilocalories per mole) Associated with the Reaction of Ti^+ with Methanol at the B3LYP/BSI//DZVP+6-311+G(2df,2p) Level[a]

products	E quartet	E doublet
$TiOH^+ + CH_3$ (**P$_1$**)	−29.5	16.8
$TiO^+ + CH_4$ (**P$_2$**)	4.0	−69.0
$TiOCH_3^+ + H$ (**P$_{3a}$**)	−10.9	16.4
$TiOHCH_2^+ + H$ (**P$_{3b}$**)	20.2	45.5
line-$TiOCH_2^+ + H_2$ (**P$_{4a}$**)	−32.3	−15.0
triangle-$TiOCH_2^+ + H_2$ (**P$_{4b}$**)	−23.1	−36.2

[a] Energies are relative to the total energy of $Ti^+(^4F)$ and methanol.

3.2. Reaction Potential Energy Surfaces. In this section, we discuss the PESs as well as the pathways for the four neutral eliminations corresponding to CH_3, CH_4, H, and H_2 in the gas-phase reaction of Ti^+ with CH_3OH, as observed in ref 10. Table 2 tabulates all possible products as well as reaction energies for these eliminations.

3.2.1. Initial C−O Activation. Initial C−O activation could account for the CH_3 and CH_4 elimination. The quartet and doublet PESs together with schematic structures involved are shown in Figure 2. Information about the relevant species is given in Figure S1 in the Supporting Information. This channel involves the classical association (**1a**). Starting from **1a**, the oxidative addition of methanol to the titanium cation accounts for $(CH_3)Ti^+(OH)$ (**2**), which stabilizes the system by 0.2 and 63.0 kcal/mol on the quartet and doublet PESs, respectively. Different from the analogous minimum $(H)Ti^+(OH)$ ($^4A''$) in the reaction of Ti^+ with H_2O, in which $\angle HTi^+O = 99.8°$,[15] the quartet new species has a linear O−Ti^+−C arrangement (178.4°) favoring electron donation to the metal center from both hydroxide-O and methyl-C 2s2p mixing orbitals as well as a decrease in repulsion between the end ligands. The arrangement of O−Ti^+−C in the doublet insertion species, however, is similar to $(H)Ti^+(OH)$ ($^2A''$) ($\angle HTi^+O = 100.1°$),[15] owing to the covalent interaction of $Ti^+(3d^24s)$ with both CH_3 and OH entities via the formation of one doubly occupied $\sigma(Ti^+C)$ and one α-singly occupied $\pi(Ti^+O)$ bonding orbital. It is this paring of metal electrons to form the covalent bonds that largely stabilizes the low-spin complex such that, compared with its precursor, the new species is featured by the reverse high- and low-spin-state order. This possibility involves a three-member ring saddle point (**TS$_{1a-2}$**) in which the C−O bond is ruptured and the Ti^+−C bond is nearly formed, as mirrored by the corresponding bond lengths. Similar to its precursor but different from its product, ^{4}**TS$_{1a-2}$** ($E_{rel} = -17.4$ kcal/mol) is more stable than ^{2}**TS$_{1a-2}$** (by 5.6 kcal/mol), and thus a crossing of the high- and low-spin surfaces is expected to occur just after the saddle point.

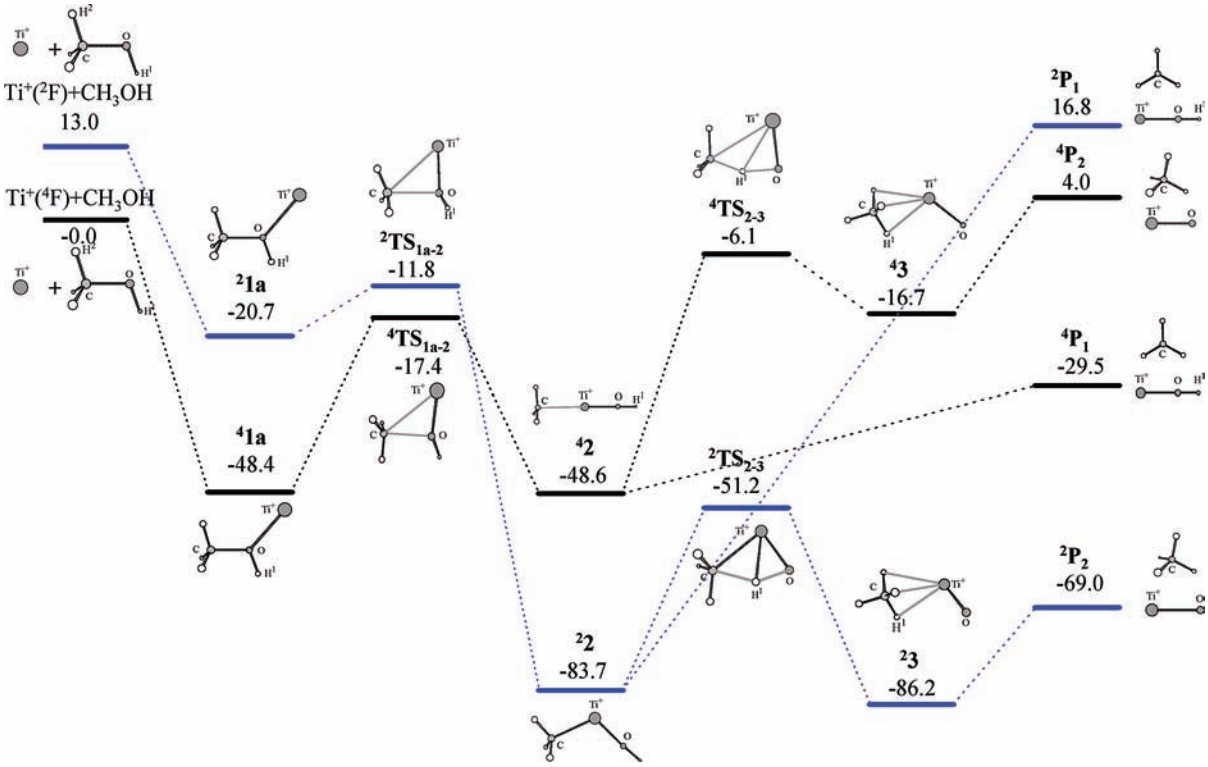

Figure 2. Energy profile for the initial C−O activation channel involved in the reaction of Ti^+ with methanol. Numbers refer to the relative energies with respect to the entrance channel of $Ti^+(^4F)$ + methanol evaluated at the B3LYP/BSI//DZVP+6-311++G(2df,2p) level including ZPE corrections. Energies are in kilocalories per mole.

The relevant MECP ($MECP_{CO}$) is located when the C−O bond length is stretched to 2.523 Å (Figure S1 in the Supporting Information), which is substantially longer than those in $\mathbf{TS_{1a-2}}$ (1.960 to 2.052 Å), suggesting that it is indeed a later crossing point. The SOCC is found to be 9.2 cm^{-1}, and the crossing probability at room temperature is estimated to be only 1%.

Once complex **2** is formed, two possible channels noticed as direct dissociation and hydroxyl-H shift dissociation could be followed. As mentioned above, the Ti^+−OH bond is stronger than the Ti^+−CH_3 bond, and direct dissociation of the latter bond in species **2** would account for the CH_3 elimination product $TiOH^+$. The overall methyl-elimination reaction is exothermic by 29.5 kcal/mol in the quartet state and endothermic by 16.8 kcal/mol in the doublet state.

Alternatively, the hydroxyl-H shift could convert species **2** into methane complex **3**, which is featured by an η^3-coordination of the methane moiety to Ti^+ with the O−Ti^+−C angle of 127.1° in ^{4}**3** and 112.1° in ^{2}**3**. NBO analysis detects that the association of OTi^+−CH_4 is dominated by electrostatic interaction as well as donor−acceptor stabilization, in which electrons are mainly donated from the coordinated C−H bonding orbitals to the metal 4s and 3d orbitals. Owing to the extremely strong $TiO^+(^2\Delta)$ bond,[36] the doublet new species is very stable, lying 86.2 kcal/mol below the energetic zero and indeed constituting the deepest energy point on the whole PES. The quartet species (E_{rel} = −16.7 kcal/mol) is highly located above its doublet state because of the large gap between the $^4\Delta$ and $^2\Delta$ states of TiO^+, as mentioned above. This possibility involves transition state $\mathbf{TS_{2-3}}$, in which the distances of the shifting H to O and C are 1.303 and 1.244 Å for the quartet state and 1.234 and 1.536 Å in the doublet state, respectively, suggesting the rupture of the O−H bond and the formation of the C−H bond. Energetically, $^4\mathbf{TS_{2-3}}$ and $^2\mathbf{TS_{2-3}}$ are located below the energetic zero by 6.1 and 51.2 kcal/mol, respectively. Homolysis of the Ti^+−C bond in species **3** would account for the methane-loss product $TiO^+(^2\Delta$ or $^4\Delta)$, which is strongly exothermic (by 69.0 kcal/mol) or endothermic by 4.0 kcal/mol with respect to the ground-state reactants. The calculated exothermicity value is in excellent agreement with the experimental estimations (71.5[38] and 68.8[11] kcal/mol).

The PES of the methane-to-methanol conversion by TiO^+, that is, the reverse reaction of the Ti^+-mediated CH_4 elimination from methanol, has been reported by Shiota and Yoshizawa using the B3LYP method in conjunction with the 6-311G** basis set for the nonmetal atoms and the (14s9p5d) primitive set supplemented with one polarization f-function for Ti.[13] In general, the feature of the reported PES is strictly identical to that presented by us; that is, the concerted pathway for the direct conversion of methane to methanol can be partitioned into the first H abstraction step and the second methyl migration step, involving a spin-inversion process between the high-spin and the low-spin PESs in the vicinity of the transition state of the second step. Moreover, comparable energetics were also obtained,[13] for example, the overall endothermicity of reaction $TiO^+(^2\Delta) + CH_4 \rightarrow Ti^+(^4F) + CH_3OH$ (72.4 kcal/mol), the binding energies of OTi^+−CH_4 (doublet) and Ti^+−(CH_3OH) (quartet) (15.4 and 51.0 kcal/mol), the doublet-to-quartet excitation energy of $(CH_3)Ti^+(OH)$ (37.0 kcal/mol), the energy barriers of the H abstraction step (corresponding to $^2\mathbf{TS_{2-3}}$ in Figure 2), and the methyl migration step (relevant to $^4\mathbf{TS_{1a-2}}$) with respect to $TiO^+(^2\Delta) + CH_4$ (16.0 and 48.7 kcal/mol).[13] However, the computation strategy employed by Shiota and Yoshizawa largely underestimates the gap of $Ti^+(^2F \leftarrow {}^4F)$ (4.3 vs 13.03 kcal/mol)[13] because of the defect of DFT in describing atomic asymptotes of transition metals;[41] and thus a substantially lower quartet-to-doublet excitation energy was reported for $Ti^+(CH_3OH)$ (10.4 kcal/mol).[13] Because the present calculation

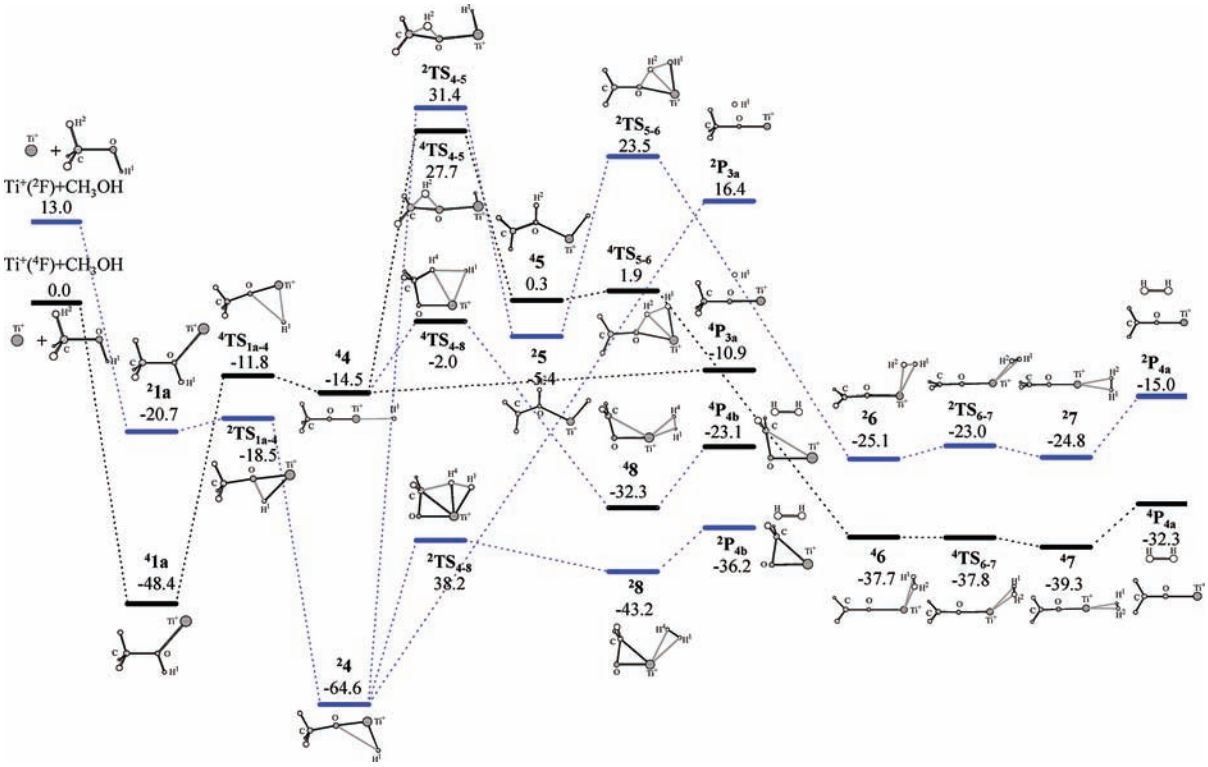

Figure 3. Energy profile for the initial O−H activation channel involved in the reaction of Ti^+ with methanol. Parameters follow the same notations as those in Figure 2.

reproduces the $Ti^+(^2F \leftarrow {}^4F)$ gap well, as mentioned above, we are confident that the PESs presented by us are more exact.

3.2.2. Initial O−H Activation. The PES together with the schematic structures involved in the channel is shown in Figure 3. Information about the involved species is given in Figure S2 in the Supporting Information. From complex **1a**, the metal could insert into the O−H bond of methanol, giving O−H insertion species **4**, which in its quartet and doublet states is 14.5 and 64.6 kcal/mol more stable than the energetic zero, respectively. Similar to the C−O insertion species discussed above, the new species is featured by perfectly linear and nearly vertical arrangements of H−Ti^+−O in the quartet and doublet states, respectively. Transition states for this possibility (^{4}**TS$_{1a-4}$** and ^{2}**TS$_{1a-4}$**) lie at 2.7 and 46.1 kcal/mol above the respective new species or 11.8 and 18.5 kcal/mol below the energetic zero. As shown in Figure 3, a quartet-to-doublet crossing is expected to occur before saddle point **TS$_{1a-4}$**. The O−H bond length in the relevant MECP ($MECP_{OH}$) is calculated to be 1.292 Å. (See Figure S2 in the Supporting Information). The SOCC is calculated to be 64.8 cm^{-1}, and the intersystem crossing probability is estimated to be 39% at room temperature, which suggests that spin-inversion occurring earlier in the process really plays an important role in the reaction mechanism.

Once species **4** is formed, three different pathways could be immediately followed, that is, direct dissociation, concerted methyl H migration, and O-mediated stepwise methyl H migration. The first pathway accounts for the H-elimination product $TiOCH_3^+$, which is exothermic with respect to the entrance channel by 10.9 kcal/mol in the quartet state and endothermic by 16.4 kcal/mol in the doublet state. The second exit of species **4** involves concerted methyl H shift accounting for dihydrogen species **8**, which is more stable than the entrance channel by 32.3 (quartet) and 43.4 (doublet) kcal/mol. This possibility involves the five-member ring transition state ^{4}**TS$_{4-8}$** and ^{2}**TS$_{4-8}$**, located at 2.0 and 38.2 kcal/mol below the entrance channel, respectively. Elimination dissociation of complex **8** would yield dehydrogenation products H_2 + triangle-$TiOCH_2^+$ (**P$_{4b}$**). The overall dehydrogenation is computed to be 23.1 (quartet) and 36.2 (doublet) kcal/mol exothermic. The last exit of species **4** corresponds to a complex, stepwise methyl H shift pathway, that is, a direct methyl H migration to oxygen forming hydroxymethyl complex **5** via transition state **TS$_{4-5}$**, a hydroxyl H shift to form dihydrogen complex **6** (via **TS$_{5-6}$**), an intracomplex rearrangement to molecular hydrogen complex **7**, and a subsequent direct dissociation giving H_2 + line-$TiOCH_2^+$ (**P$_{4a}$**). This channel is energetically unfavorable because the involved transition states (^{4}**TS$_{4-5}$**, ^{2}**TS$_{4-5}$**, and ^{2}**TS$_{5-6}$**) are highly located on the PES.

3.2.3. Initial C−H Activation. Calculated PES together with schematic structures involved in the channel are shown in Figure 4. Information about the involved species is given in Figure S3 in the Supporting Information. We can find that the reaction could occur through both encounter complexes **1a** and **1b**. Oxidative addition of the metal ion across the C−H bond in **1a** and **1b** accounts for hydride-containing species **9** and **9b**, respectively; the quartet (doublet) transition state **TS$_{1a-9}$** (for **1a** → **9** conversion) lies at 2.5 (5.3) kcal/mol below the energetic zero, whereas **TS$_{1b-9b}$** (for **1b** → **9b** conversion) is located at 14.9 (quartet) and 13.5 (doublet) kcal/mol above the energetic zero. In the new minima **9** and **9b**, TiH^+ simultaneously attaches via the metal to both the C and O atoms of CH_2OH, with the main difference in the orientation of Ti^+H axis. Energetically, **9** and **9b** are nearly degenerate in both the doublet and quartet states, and the doublet species **9** and **9b** ($E_{rel} \approx -33.0$ kcal/mol) are much more stable than the quartet analogues (by about 28 kcal/mol). To clarify the stability of the hydride-containing species in the different states, we select species **9** to be a model for our study. NBO analysis indicates that the quartet species favors only donor−acceptor interactions between Ti^+H^2 and CH_2OH entities; and the larger stability of the doublet species

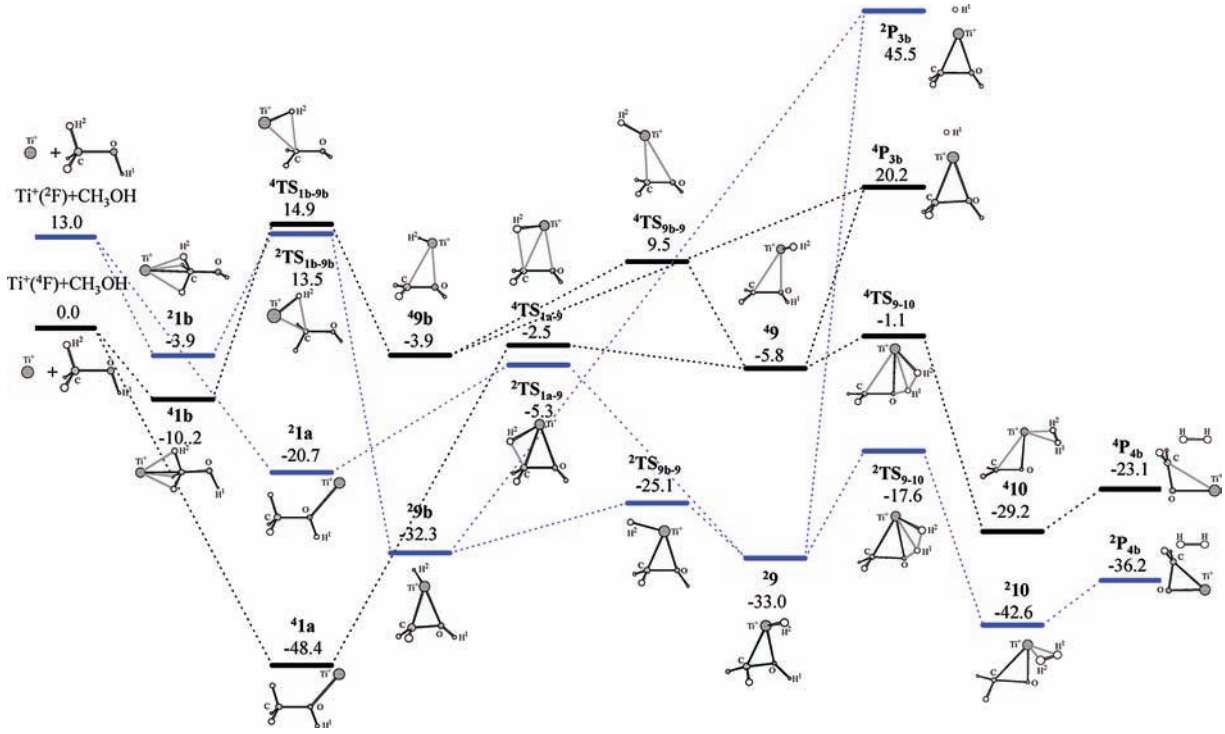

Figure 4. Energy profile for the initial C−H activation channel involved in the reaction of Ti^+ with methanol. Parameters follow the same notations as those in Figure 2.

results from one doubly occupied $\sigma(Ti^+C)$ orbital as well as electron donation from the 2s2p(O) hybridized orbital to the metal 4s3d hybridized and $\sigma^*(Ti^+H^2)$ orbitals. Hydride-containing species **9** and **9b** could convert into each other; the relevant transition state ($\mathbf{TS_{9b-9}}$) lies at 9.5 (−25.1) kcal/mol on the quartet (doublet) PES. Similar to the O−H activation process discussed above, a nonadiabatic crossing between the quartet and doublet PESs is experienced before the respective C−H insertion transition states from both encounter complexes.

Both **9** and **9b** could directly decompose into product $TiOHCH_2^+$ + H ($\mathbf{^4P_{3b}}$ or $\mathbf{^2P_{3b}}$) with high appearance energy (lying at 20.2 or 45.5 kcal/mol above the entrance channel). The other exit of species **9** is the subsequent hydroxide-H abstraction leading to molecular hydrogen complex **10**. The relevant transition states $\mathbf{^4TS_{9-10}}$ and $\mathbf{^2TS_{9-10}}$ are calculated to be 1.1 and 17.6 kcal/mol below the entrance channel, respectively. The new species is located at −29.2 kcal/mol in the quartet state and −42.6 kcal/mol on the doublet PES. Along both the quartet and doublet coordinates, species **10** would eventually dissociate into dehydrogenation products H_2 + triangle-$TiOCH_2^+$ ($\mathbf{P_{4b}}$) with the overall exothermicities of 23.1 and 36.2 kcal/mol, respectively.

3.3. Reaction Mechanisms. In this section, we summarize the reaction mechanisms of Ti^+ with methanol by comparing our theoretical results with the findings from the SIDT-LV and LA−MB experiments.[10,11]

In the SIDT-LV experiment,[10] because most of the metal cations generated with the laser vaporization source are in the ground state $Ti^+(a^4F)$, the reaction with CH_3OH should correspond to the ground-state chemistry, which gives TiO^+, $TiOH^+$, $TiOCH_2^+$, and $TiOCH_3^+$, with $TiOH^+$ accounting for over 50% of the overall products. These products can be classified as two groups: loss of a radical-type species (H or CH_3) and loss of a closed-shell molecule (H_2 or CH_4). In the LA−MB experiment,[11] the products associated with H, CH_3, and CH_4 elimination were also observed for the reaction of Ti^+-methanol heteroclusters, and the H elimination was suggested to involve O−H bond activation by isotope-labeling experiments.

In the present theoretical investigation, all possible pathways starting with C−O, C−H, and O−H activation are searched for the reaction of Ti^+ with methanol. Methane and methyl loss products (TiO^+ and $TiOH^+$) are produced via initial C−O activation (Figure 2), whereas initial O−H and C−H activation account for the H_2 and H elimination ($TiOCH_2^+$ and $TiOCH_3^+$). (See Figures 3 and 4.) In all cases, there is a crossing between the high- and low-spin-state energy surfaces in the course of initial bond insertion; and the crossing is located somewhere before the transition state for the X−H (X = C and O) insertion and after the C−O insertion transition state. This phenomenon can be explained by the fact that the stability of the low-spin insertion complexes is enhanced by the formation of two M−L bonds through the pairing of two metal electrons with two electrons originally occupying the X−H or C−O σ bond. An analogous situation has also been found in the reaction of M^+ (M = Sc, Ti, and Cr) with NH_3 and H_2O[14−17,19] as well as in the V^+, Nb^+, or Ta^+ reaction with methanol.[9]

If the spin inversion is not considered, then initial C−O activation is energetically the most favorable because of the lowest energy barrier involved. Along this coordinate, CH_3 elimination affording $TiOH^+$ ($\mathbf{^4P_1}$) from the C−O insertion minimum ($\mathbf{^42}$) is expected to be very favored because it involves a simple bond insertion−reductive elimination pathway as well as the single-state reactivity (SSR) paradigm, which explains the SIDT-LV experimental finding that $TiOH^+$ accounts for over 50% of the overall products.[10] For the CH_4 elimination, because the estimated crossing probability due to SOC in the course of the C−O activation is too low (1%) to account for all of the product of TiO^+ in the SIDT-LV experiment,[10] the excited state ($\mathbf{^4P_2}$) should become accessible with excess energies, even though it is a little endothermic. It is the high location of the product channel that explains the minor production of TiO^+, as observed in the experiment.[10]

Although both initial C−H and O−H activation could be responsible for the elimination of H and H_2, the former is unlikely to be important on the basis of the following facts: (1) transition states for initial C−H activation starting from both classical complex **1a** (almost isoergetic to the ground-state reactants) and nonclassical complexes **1b** (highly above the ground-state reactants) are higher in energy than those for initial O−H activation by 9.3 kcal/mol and as large as 26.7 kcal/mol; (2) the strongly endothermic H elimination product $TiOHCH_2^+$ (**P_{3b}**) from the C−H activation pathway (by at least 20 kcal/mol; see Figure 4) cannot explain the findings of the SIDT-LV experiment;[10] (3) the reaction of Ti^+ with $(CH_3OD)_n$ in the LA−MB experiment did not afford product ions corresponding to TiD^+ and $TiODCH_2^+$.[11]

Along the initial O−H activation pathway, similar to the loss of methyl as mentioned above, the H elimination giving $TiOCH_3^+$ (**P_{3a}**) is also likely to take place adiabatically on the quartet PES through the simple bond insertion−reductive elimination mechanism because all of the stationary points involved are located far below the entrance channel, whereas the product on the doublet PES (^{2}**P_{3a}**) is highly endothermic. (See Figure 3.) However, the O−H bond insertion−stepwise methyl H shift−reductive elimination pathway can be rule out for the H_2 loss because of several high-energy barriers involved, and the H_2 loss is more likely to occur through the O−H bond insertion−concerted methyl H shift−reductive elimination pathway. Therefore, the H_2 loss product is triangle-$TiOCH_2^+$ (**P_{4b}**) rather than line-$TiOCH_2^+$ (**P_{4a}**). As mentioned above, the spin inversion in the course of the O−H activation should play an important role in the product channel because it involves a large crossing probability (39%). Thanks to the spin inversion, the reaction could take place on both the high- and low-spin PESs because they are both energetically accessible.

In summary, for the reaction of $Ti^+(a^4F)$ with methanol, the loss of a radical-type species (H or CH_3) takes place adiabatically on the quartet PES via the simple bond insertion−reductive elimination mechanism, and the loss of a closed-shell molecule (H_2 or methane), which involves the bond insertion−H shift−reductive elimination mechanism, could take place on both the quartet and the doublet PESs because of a spin inversion in the course of the bond insertion process. The major product of TiO^+ observed in the SIDT-LV experiment[10] is consistent with the relatively low C−O insertion energy barrier as well as the SSR paradigm.

4. Conclusions

The gas-phase reaction of Ti^+ with methanol has been theoretically investigated. We can now conclude by summarizing a number of main points: (1) The approach of Ti^+ to CH_3OH could account for two types of encounter complexes: "classical" O− (**1a**) or "nonclassical" methyl H-attached complex (**1b**). The classical association accounts for rather strong binding, whereas a relatively weak bond is formed in the nonclassical complex. The reaction of Ti^+ with CH_3OH takes place via the formation of the classical association rather than the nonclassical complex. (2) All possible pathways starting with C−O, C−H, and O−H activation have been searched. Methane and methyl loss products (TiO^+ and $TiOH^+$) are produced via the initial C−O activation; the initial O−H activation accounts for the H_2 and H elimination products ($TiOCH_2^+$ and $TiOCH_3^+$), and the initial C−H activation is unlikely to be important in the chemistry of Ti^+ with methanol. (3) In all cases, there is a crossing between the high- and low-spin-state energy surfaces in the course of the initial bond insertion, and the crossing is located somewhere before the transition states for the X−H (X = C and O) insertion and after the C−O insertion transition state. The loss of a closed-shell molecule (H_2 or methane) channel involving the bond insertion−H shift−reductive elimination mechanism could take place on both the quartet and doublet PESs thanks to the spin inversion, whereas the loss of a radical-type species (H or CH_3) is produced adiabatically on the quartet PES through the simple bond insertion−reductive elimination mechanism. The major product of $TiOH^+$ observed in the SIDT-LV experiment[10] is the result of the relatively low C−O insertion energy barrier as well as the SSR paradigm.

Acknowledgment. This work was supported by NCET-05-0608, and Program for Changjiang Scholars and Innovative Research Team in University (IRT0759) of MOE, PRC, NSFC (20476061), and State Key Basic Research Program of China (2006CB202505).

Supporting Information Available: Optimized structures as well as selected structural parameters for all the intermediates, MECP, saddle points and products involved in the loss of H_2, H, CH_3, and CH_4, and calculated total energies, and zero-point energies, and values of $<S^2>$ for all the relevant species. This material is available free of charge via the Internet at http://pubs.acs.org.

References and Notes

(1) (a) Yamane, H.; Mabumoto, H.; Hirai, T. *Appl. Phys. Lett.* **1988**, *53*, 1548. (b) Hubert-Pfalzgraf, L. G. *New J. Chem.* **1995**, *19*, 727. (c) Bradley, D. C. *Chem. Rev.* **1989**, *89*, 1317.

(2) (a) Allison, J.; Ridge, D. P. *J. Phys. Chem.* **1976**, *98*, 7445. (b) Allison, J.; Ridge, D. P. *J. Phys. Chem.* **1977**, *100*, 163. (c) Jone, R. W.; Staley, R. H. *J. Phys. Chem.* **1982**, *86*, 1669. (d) Tsarbopoulos, A.; Allison, J. *J. Am. Chem. Soc.* **1985**, *107*, 5085. (e) Prűsse, T.; Schwarz, H. *Organometallics* **1989**, *8*, 2856. (f) Karrass, S.; Prűsse, T.; Eller, K.; Schwarz, H. *J. Am. Chem. Soc.* **1989**, *111*, 9018. (g) Chen, Y. M.; Clemmer, D. E.; Armentrout, P. B. *J. Am. Chem. Soc.* **1994**, *116*, 7815. (h) Wesendrup, R.; Schalley, C. A.; Schröder, D.; Schwarz, H. *Organometallics* **1996**, *15*, 1435. (i) Kirkwood, D. A.; Stace, A. J. *J. Am. Chem. Soc.* **1998**, *120*, 12316.

(3) Allison, J.; Ridge, D. P. *J. Phys. Chem.* **1979**, *101*, 4998.

(4) Huang, S.; Holman, R. W.; Gross, M. L. *Organometallics* **1986**, *5*, 1857.

(5) Weil, D. A.; Wilkins, C. L. *J. Am. Chem. Soc.* **1985**, *107*, 7316.

(6) Eller, K.; Schwarz, H. *Chem. Rev.* **1991**, *91*, 1121.

(7) Azzaro, M.; Breton, S.; Decouzon, M.; Geribaldi, S. *Int. J. Mass Spectrom. Ion Processes* **1993**, *128*, 1.

(8) Lu, W. Y.; Yang, S. H. *J. Phys. Chem. A* **1998**, *102*, 825.

(9) Cao, Y. L.; Zhao, X.; Xin, B.; Xiong, S. X.; Tang, Z. C. *J. Mol. Struct.* **2004**, *683*, 141.

(10) Guo, B. C.; Kerns, K. P.; Castleman, A. W. *J. Phys. Chem.* **1992**, *96*, 4879.

(11) Koo, Y. M.; Kim, J. H.; Choi, Y. K.; Lee, H.; Jung, K. W. *J. Phys. Chem. A* **2002**, *106*, 2465.

(12) Stöckigt, D. *J. Phys. Chem. A* **1998**, *102*, 10493.

(13) Shiota, Y.; Yoshizawa, K. *J. Am. Chem. Soc.* **2000**, *122*, 12317.

(14) Irigoras, A.; Fowler, J. E.; Uglade, J. M. *J. Am. Chem. Soc.* **1999**, *121*, 574.

(15) Irigoras, A.; Fowler, J. E.; Uglade, J. M. *J. Chem. Phys. A* **1998**, *102*, 293.

(16) Schwarz, H. *Int. J. Mass Spectrom.* **2004**, *237*, 75.

(17) Sicilia, E.; Russo, N. *J. Am. Chem. Soc.* **2002**, *124*, 1471.

(18) Zhao, L. M.; Zhang, R. R.; Guo, W. Y.; Lu, X. Q. *Chem. Phys. Lett.* **2006**, *431*, 56.

(19) Russo, N.; Sicilia, E. *J. Am. Chem. Soc.* **2001**, *123*, 2588.

(20) (a) Stephens, P. J.; Devlin, F. J.; Chabalowski, C. F.; Frisch, M. J. *J. Phys. Chem.* **1994**, *98*, 11623. (b) Becke, A. D. *J. Chem. Phys.* **1993**, *98*, 5648.

(21) (a) Lee, C.; Yang, W.; Parr, R. G. *Phys. Rev. B* **1988**, *37*, 785. (b) Salahub, D. R. *In The Challenge of d and f Electrons*; Zerner, M. C., Ed.; American Chemical Society: Washington, DC, 1989. (c) Parr, R. G.; Yang, W. *Density-Functional Theory of Atoms and Molecules*; Oxford University Press: Oxford, U.K., 1989.

(22) Chiodo, S.; Russo, N.; Sicilia, E. *J. Comput. Chem.* **2005**, *26*, 175.

(23) Chiodo, S.; Kondakova, O.; Michelini, M. C.; Russo, N.; Sicilia, E. *J. Phys. Chem. A* **2004**, *108*, 1069.

(24) Wachters, A. J. *J. Chem. Phys.* **1970**, *52*, 1033.
(25) Hay, P. J. *J. Chem. Phys.* **1971**, *66*, 4377.
(26) Raghavachari, K.; Trucks, G. W. *J. Chem. Phys.* **1989**, *91*, 1062.
(27) Frisch, M. J.; Trucks, G. W.; Schlegel, H. B.; Scuseria, G. E.; Robb, M. A.; Cheeseman, J. R.; Montgomery, J. A., Jr.; Vreven, T.; Kudin, K. N.; Burant, J. C.; Millam, J. M.; Iyengar, S. S.; Tomasi, J.; Barone, V.; Mennucci, B.; Cossi, M.; Scalmani, G.; Rega, N.; Petersson, G. A.; Nakatsuji, H.; Hada, M.; Ehara, M.; Toyota, K.; Fukuda, R.; Hasegawa, J.; Ishida, M.; Nakajima, T.; Honda, Y.; Kitao, O.; Nakai, H.; Klene, M.; Li, X.; Knox, J. E.; Hratchian, H. P.; Cross, J. B.; Adamo, C.; Jaramillo, J.; Gomperts, R.; Stratmann, R. E.; Yazyev, O.; Austin, A. J.; Cammi, R.; Pomelli, C.; Ochterski, J. W.; Ayala, P. Y.; Morokuma, K.; Voth, G. A.; Salvador, P.; Dannenberg, J. J.; Zakrzewski, V. G.; Dapprich, S.; Daniels, A. D.; Strain, M. C.; Farkas, O.; Malick, D. K.; Rabuck, A. D.; Raghavachari, K.; Foresman, J. B.; Ortiz, J. V.; Cui, Q.; Baboul, A. G.; Clifford, S.; Cioslowski, J.; Stefanov, B. B.; Liu, G.; Liashenko, A.; Piskorz, P.; Komaromi, I.; Martin, R. L.; Fox, D. J.; Keith, T.; Al-Laham, M. A.; Peng, C. Y.; Nanayakkara, A.; Challacombe, M.; Gill, P. M. W.; Johnson, B.; Chen, W.; Wong, M. W.; Gonzalez, C.; Pople, J. A. *Gaussian 03*, revision B.05; Gaussian, Inc.: Pittsburgh, PA, 2003.
(28) Schmidt, M. W.; Baldridge, K. K.; Boatz, J. A.; Elbert, S. T.; Gordon, M. S.; Jensen, J. H.; Koseki, S.; Matsunaga, N.; Nguyen, K. A.; Su, S. J.; Windus, T. L.; Dupuis, M.; Montgomery, J. A. *J. Comput. Chem.* **1993**, *14*, 1347.
(29) Matsunaga, N.; Koseki, S.; Gordon, M. S. *J. Chem. Phys.* **1996**, *104*, 7988.
(30) Fedorov, D. G.; Koseki, S.; Schmidt, M. W.; Gordon, M. S. *Int. Rev. Phys. Chem.* **2003**, *22*, 551.
(31) (a) Zener, C. *Proc. R. Soc. London, Ser. A* **1932**, *137*, 595. (b) Zener, C. *Proc. R. Soc. London, Ser. A* **1933**, *140*, 1174. (c) Fedorov, D. G.; Koseki, S.; Schmidt, M. W.; Gordon, M. S. *Int. Rev. Phys. Chem.* **2003**, *22*, 551.
(32) Glendening, E. D.; Badenhoop, J. K.; Reed, A. E.; Carpenter, J. E.; Bohmann, J. A.; Morales, C. M.; Weinhold, F. *NBO5.0*; Theoretical Chemistry Institute, University of Wisconsin: Madison, WI, 2001.
(33) Kimura, K.; Kubo, M. *J. Chem. Phys.* **1959**, *30*, 151.
(34) Rodgers, M. T.; Armentrout, P. B. *J. Phys. Chem. A* **1999**, *103*, 4955.
(35) Moore, C. E. *Atomic Energy Levels*; NSRD-NBS, U.S. Government Printing Office: Washington, DC, 1991; Vol. 1.
(36) Fisher, E. R.; Elkind, J. L.; Clemmer, D. E.; Georgiadis, R.; Loh, S. K.; Aristov, N.; Sunderlin, L. S.; Armentrout, P. B. *J. Chem. Phys.* **1990**, *93*, 2676.
(37) Chen, Y. M.; Clemmer, D. E.; Armentrout, P. B. *J. Phys. Chem.* **1994**, *98*, 11490.
(38) Clemmer, D. E.; Aristov, N.; Armentrout, P. B. *J. Phys. Chem.* **1993**, *97*, 544.
(39) Alessandra, R.; Bauschlicher, C. W., Jr. *J. Phys. Chem. A* **1997**, *101*, 8949.
(40) Sunderlin, L. S.; Armentrout, P. B. *J. Phys. Chem.* **1988**, *92*, 1209.
(41) Ziegler, T.; Li, J. *Can. J. Chem.* **1994**, *72*, 783.

JP901326R